Synthetic and Computer-Assisted Analysis of the Structural Requirements for Selective, High-Affinity Ligand Binding to Diazepam-Insensitive Benzodiazepine Receptors

Garry Wong,*,† Konrad F. Koehler,*,‡ Phil Skolnick,† Zi-Qiang Gu,† Subramaniam Ananthan,§ Peter Schönholzer,∥ Walter Hunkeler,∥ Weijiang Zhang,⊥ and James M. Cook⊥

Laboratory of Neuroscience, National Institute of Diabetes and Digestive and Kidney Diseases, National Institutes of Health, Bethesda, Maryland 20892, Drug Design Section, Searle Research and Development, Skokie, Illinois 60077, Organic Chemistry Research Department, Southern Research Institute, Birmingham, Alabama 35255, Pharma Division, Preclinical Research, F. Hoffmann-La Roche Ltd., Basel, Switzerland, and Department of Chemistry, University of Wisconsin—Milwaukee, Milwaukee, Wisconsin 53201

Received November 30, 1992

Several 1,4-diazepines were recently reported to bind with high affinities to the "diazepam-insensitive" (DI) isoform of the benzodiazepine receptor (BzR) (Korpi, E. R.; Uusi-Oukari, M.; Wegelius, K. *Eur. J. Pharm.* **1992**, *213*, 323–329. Wong, G.; Skolnick, P. *Eur. J. Pharmacol. Mol. Pharm. Sec.* **1992**, *225*, 63–68). However, only the putative ethanol antagonist 1 (Ro 15-4513) displayed modest selectivity for the DI site compared to other "diazepam-sensitive" (DS) BzR isoforms. In order to probe the requirements for selective, high-affinity binding to the DI site, the affinities of 47 benzodiazepines have been determined at both DI and DS BzR sites. In addition, single X-ray crystallographic analyses for three of these derivatives, **5** (Ro 17-1812), **6** (Ro 16-6028), and **42** (Ro 14-5974), are reported. The radioligand binding studies reveal that modifications to the 3-, 7-, and 8-positions of 6-oxoimidazo[1,5-*a*][1,4]benzodiazepines have a marked influence on the K_i(DI)/K_i(DS) ratios. In order to more precisely determine the structural requirements for both high affinity and selectivity at DI BzR relative to DS, 3D-QSAR analyses were carried out on ligand affinities at both of these BzR isoforms. This analysis was based, in part, on the new X-ray crystallographic data. Satisfactory cross-validated regression equations were obtained individually for the logarithms of ligand affinities at DI and DS as well as for the differences of the logarithms of their affinities at these two isoforms (cross-validated $R^2 > 0.70$ for all three regression equations). The steric and electrostatic 3D-QSAR DI and DS maps are in qualitative accord with the structure–activity relationship (SAR) data. Furthermore, the DI and DI/DS maps may be useful in the design of ligands with enhanced DI affinity and DI/DS selectivity, respectively.

Introduction

$GABA_A$/benzodiazepine receptors (BzR) are a hetero-oligomeric group of ligand-gated ion channels that constitute the major inhibitory neurotransmitter system in the mammalian CNS.[1] Ligands acting through benzodiazepine receptors (BzR) elicit a wide range of pharmacological effects including sedation, muscle relaxation, anxiolytic, and anticonvulsant activities.[1] Molecular biological and physiological studies have established that at least two of the three different subunits (α, β, γ) are necessary to constitute a functional receptor which mimics many of the pharmacological, biochemical, and electrophysiological properties of native receptors.[2,3] The identification of multiple α, β, and γ subunits raises the possibility that very large numbers of $GABA_A$ receptor isoforms may be present in the CNS.[4]

The "diazepam-insensitive" (DI) subtype of benzodiazepine receptor (BzR) was initially described in rodent cerebellar membranes and cerebellar granule cell cultures.[5,6] The DI BzR represent 25-30% of cerebellar BzR but is only a very minor constituent (0-5%) in other regions of the mammalian central nervous system.[7] DI are characterized by the low affinity (> 1 μM) of prototypical 1,4-benzodiazepines (e.g., diazepam, flunitrazepam), some β-carbolines (e.g., 3-carbomethoxy-β-carboline), triazolobenzodiazepines (e.g., triazolam), and triazolopyridazines (e.g., CL 218872) that are high affinity ligands at other "diazepam-sensitive" (DS) BzR isoforms.[7-10] These findings support the hypothesis that DI BzR represents a distinct subtype with more restrictive ligand binding requirements than other BzR isoforms. A pharmacological profile similar to that of the native DI BzR can be reconstituted in cell cultures transfected with cDNA's encoding an α6, β2, γ2 subunit configuration.[11] DS BzR can be reconstituted with any one of α1–3 or -5 together with β2 and γ2 subunits.[12]

The DI BzR is of particular interest since the imidazodiazepines 1 (Ro 15-4513), 2 (Ro 15-3505), and 3 (Ro 19-4603) possess high affinities (K_i < 60 nM) for this isoform.[8] These three compounds were previously shown to antagonize some of the behavioral and biochemical effects of ethanol.[13-15] These findings, coupled with a recent report which demonstrated that alcohol nontolerant (ANT) rats lack DI receptors, suggest that the DI BzR may play a role in the ability of these compounds to reverse some of the neurochemical and behavioral effects of

† Laboratory of Neuroscience, National Institute of Diabetes and Digestive and Kidney Diseases, National Institutes of Health.
‡ Drug Design Section, Searle Research and Development; inquiries concerning the computer modeling aspects of this paper should be directed to this author. Present address: Istituto di Ricerche di Biologia Molecolare (IRBM), 00040 Pomezia (Roma), Italy.
§ Organic Chemistry Research Department, Southern Research Institute.
∥ Pharma Division, Preclinical Research, F. Hoffmann-La Roche Ltd.
⊥ Department of Chemistry, University of Wisconsin—Milwaukee.

0022-2623/93/1836-1820$04.00/0

Table I. Affinity of 5,6-Dihydro-5-methyl-6-oxo-4*H*-imidazo[1,5-*a*][1,4]benzodiazepine-3-carboxylic Acid Derivatives for the DS and DI Benzodiazepine Receptors

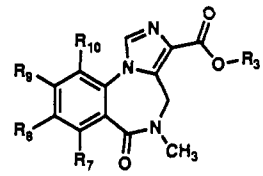

compound	R_3	R_7	R_8	R_9	R_{10}	DS (nM)[a]	DI (nM)[a]	DI/DS
1[c] (Ro 15-4513)	CH_2CH_3		N_3			5.3 ± 1.2	3.1 ± 0.1	0.6
2[c] (Ro 15-3505)	CH_2CH_3	Cl				0.2 ± 0.0	20 ± 2.4	100
4[c] (Ro 15-1788)	CH_2CH_3		F			0.8 ± 0.1	58 ± 11	73
7[d]	CH_3		F			3.1 ± 1.4	239 ± 32	77
8[d]	CH_3					6.3	1409	224
9[c] (Ro 14-7437)	CH_2CH_3					1.3 ± 0.1	214 ± 4.0	165
10[d]	$C(CH_3)_3$					1.1 ± 0.1	21.2 ± 4.0	19.2
11[d]	CH_3		Cl			29.8 ± 5.4	123.5 ± 1.8	4.1
12[d] (Ro 15-1310)	CH_2CH_3		Cl			5.4 ± 0.9	16.9 ± 1.1	3
13[d]	$CH_2CH_2CH_3$		Cl			24.8 ± 1.4	33.3 ± 2.3	1.3
14[d]	$CH(CH_3)_2$		Cl			10.5 ± 1.1	8.8 ± 1.0	0.8
15[d]	cyclopropylmethyl		Cl			9.7 ± 1.8	39.8 ± 7.9	4.1
16[d]	$C(CH_3)_3$		Cl			4.0 ± 0.9	1.7 ± 0.3	0.4
17[d]	$CH(CH_2CH_3)_2$		Cl			26.9 ± 9.2	122.6 ± 11.7	4.6
18[d]	$CH_2C(CH_3)_3$		Cl			499.3 ± 37.1	299.6 ± 28.0	0.67
19[d]	$CH_2CH_2C(CH_3)_3$		Cl			184 ± 1.4	>1000	
20 (Ro 15-5623)	CH_2CH_3	F				0.8 ± 0.1	102 ± 14	128
21 (Ro 15-1746)	CH_2CH_3			Cl		>1000	>10000	
22 (Ro 15-3237)	CH_2CH_3				Cl	>1000	>10000	

[a] Values (K_i) for new compounds are listed with statistical limits and represent $\bar{X}$ ± SEM ≥ 3 experiments except for 8 (one experiment). [b] K_d value. [c] See ref 8 for details. [d] See ref 37 for details.

ethanol.[6] The ability of high-affinity DI ligands to produce a discriminative stimulus in pigeons trained to the imidazodiazepinone 4 (Ro 15-1788) provided additional evidence that behavior can be effected through DI BzR.[9] A better understanding of the ligand requirements for binding to DI and to DS should aid in the design and synthesis of more selective and higher affinity DI ligands which may in turn serve to further elucidate the physiological and pharmacological functions of this unique $GABA_A$ receptor isoform.

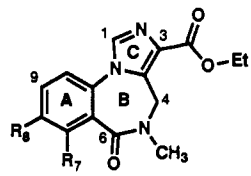

1 (Ro 15-4513); R_7 = H, R_8 = N_3
2 (Ro 15-3505); R_7 = Cl, R_8 = H
4 (Ro 15-1788); R_7 = H, R_8 = F

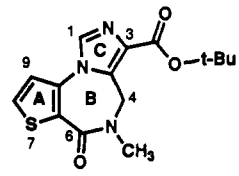

3 (Ro 19-4603)

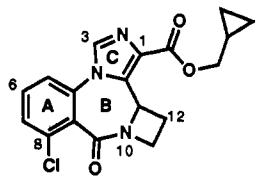

5 (Ro 17-1812)

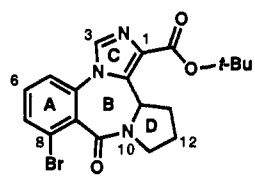

6 (Ro 16-6028)

The structure–affinity relationships of several 1,4-diazepines [e.g., 5 (Ro 17-1812) and 6 (Ro 16-6028)] containing one or more annelated ring systems for their affinities at DI BzR were recently described.[8,10] We have now extended these studies by evaluating additional 1,4-diazepines and performed excluded volume[16,17] and CoMFA (comparative molecular field analysis)[18] studies to ascertain the determinants for selective, high-affinity binding to DI BzR.

Computer Modeling Methods

General. The CONCORD,[19-21] MOLGRAF,[22] and ESPFIT[23] calculations were run on VAX 6430 minicomputer. The Gaussian 90[24] calculations were performed on a Cray X-MP supercomputer while the Gaussian 92[25] optimizations were carried out on an IBM RS-6000 Model 560 workstation. Finally, Sybyl[21] and MacroModel[26,27] calculations were done on a Silicon Graphics Personal Iris 4D/35.

3D-QSAR. The starting geometries of the 6-oxo-imidazo[1,5-*a*][1,4]benzodiazepines (Table I) were constructed from the X-ray crystal structure of 4 (Ro 15-1788)[28,29] and modified where necessary using the fragment library of Sybyl version 5.5. In the case of the 9-oxo-imidazo[1,5-*a*]pyrrolo[2,1-*c*][1,4]benzodiazepines (Table III, compounds **6, 34-42**), the geometry of the pyrrolo ring was taken from the X-ray structure of 1,2,3,10,11,11a-hexahydro-5*H*-pyrrolo[2,1-*c*][1,4]benzodiazepine (**49**).[30] The geometries of flexible side chains and hydrogen atoms were minimized using MM2 (molecular mechanics program 2) force field[31] in MacroModel version 3.5 holding the heterocyclic core fixed. The structures which resulted were then subjected to ab initio 3-21G energy minimization using the Gaussian 92 program. All bond lengths and valence angles were optimized while holding the torsional angles fixed. The ab initio geometry optimizations were followed by a single point 6-31G* calculation (SCF= TIGHT convergence criteria). Electrostatic potential fit charges were calculated using the ab initio 6-31G* wave function and the ESPFIT program based upon the Kollman et al. algorithm.[32]

The CoMFA[18] study was performed using the QSAR module of SYBYL version 5.5. Unless specifically stated otherwise, default settings were used throughout. The centroid of the ring A of 1 (Ro 15-4513) was placed at the origin, and the molecule was rotated to place the A ring in the $X-Y$ plane. The remainder of the molecules were

Table II. Affinity of 5,6-Dihydro-5-alkyl-6-oxo-4*H*-imidazo[1,5-*a*][1,4]benzodiazepine Derivatives for the DS and DI Benzodiazepine Receptors

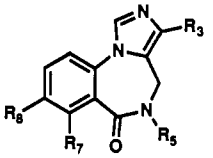

compound	R_3	R_5	R_7	R_8	DS (nM)[a]	DI (nM)[a]	DI/DS
23[b]	$CO_2CH_2CH_3$	$CH_2CH{=}CH_2$	H	H	39.2 ± 9.9	1132 ± 119	29
24[b]	$CO_2CH_2CH_3$	$CH_2C_6H_5$	H	Cl	13.7 ± 1.3	10.9 ± 1.4	0.8
25[b]	$CO_2CH_2CH_3$	$CH_2C_6H_5$	Cl	H	0.4 ± 0.1	20.2 ± 0.9	51
26[b]	3Me124Ox[c]	$CH_2C_6H_5$	Cl	H	7.5 ± 1.6	761 ± 184	101
27[b]	3Me124Ox[c]	$CH_2C_6H_5$	H	Cl	88.4 ± 5.7	115 ± 7.3	1.3
28[b]	$CO_2CH_2CH_3$	$CH_2C_6H_5$	H	H	1.5 ± 0.1	112 ± 8.1	75
29[b]	3Me124Ox[c]	$CH_2C_6H_5$	H	H	907.1 ± 111	>10000	
30[b]	5Me134Ox[d]	$CH_2C_6H_5$	H	H	1209 ± 118	>10000	

[a] Values for new compounds are listed with statistical limits and represent $\bar{X}$ ± SEM ≥ 3 experiments. [b] See ref 38 for details.

[c] 3Me124Ox =  [d] 5Me134Ox = 

Table III. Affinity of 12,12a-Dihydro-9-oxo-9*H*,11*H*-azeto[2,1-c]imidazo[1,5-*a*][1,4]benzodiazepine-1-carboxylic Acid and 11,12,13,13a-Tetrahydro-9-oxo-9*H*-imidazo[1,5-*a*]pyrrolo[2,1-c][1,4]benzodiazepine-1-carboxylic Acid Derivatives for the DS and DI Benzodiazepine Receptors

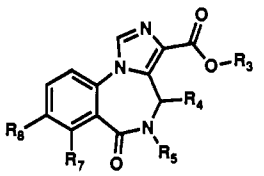

compound	R_3	R_4	R_5	R_7	R_8	DS (nM)[a]	DI (nM)[a]	DI/DS
5[b] (Ro 17-1812)	cyclopropylmethyl	$-CH_2CH_2-$		Cl		0.1 ± 0.0	55 ± 3.0	554
31 (Ro 16-0858)	CH_2CH_3	$-CH_2CH_2-$		Cl		0.2 ± 0.0	34.0 ± 2.0	170
32 (Ro 16-0153)	$C(CH_3)_3$	$-CH_2CH_2-$		Cl		1.1 ± 1.2	15.0 ± 2.1	14
33 (Ro 17-2620)	$C(CH_3)_3$	$-CH_2CH_2-$			F	1.8 ± 0.1	16.9 ± 1.0	9
6[b] (Ro 16-6028)	$C(CH_3)_3$	$-CH_2CH_2CH_2-$		Br		0.5 ± 0.1	10.0 ± 2.0	20
34 (Ro 16-3607)	$C(CH_3)_3$	$-CH_2CH_2CH_2-$		OCH_3		5.1 ± 1.0	259.4 ± 17	51
35 (Ro 16-6624)	$C(CH_3)_3$	$-CH_2CH_2CH_2-$		CH_2CH_3		1.0 ± 0.1	163.7 ± 32	164
36 (Ro 15-4941)	CH_2CH_3	$-CH_2CH_2CH_2-$		Cl		0.2 ± 0.0	68.8 ± 4.3	344
37 (Ro 16-6127)	$C(CH_3)_3$	$-CH_2CH_2CH_2-$		Cl	F	1.0 ± 0.1	23.6 ± 3.1	24
38[c] (Ro 14-5975)	CH_2CH_3	$-CH_2CH_2CH_2-$			Cl	72.6 ± 40	53.8 ± 7.7	0.7
39 (Ro 16-3058)	$C(CH_3)_3$	$-CH_2CH_2CH_2-$			Cl	65.2 ± 15	26.8 ± 1.1	0.4
40 (Ro 17-3128)	cyclohexyl	$-CH_2CH_2CH_2-$			Cl	391 ± 47	165 ± 6	0.42
41 (Ro 17-3129)	cyclopropylmethyl	$-CH_2CH_2CH_2-$			Cl	378 ± 100	81 ± 4	0.22
42[c] (Ro 14-5974)	CH_2CH_3	$-(S)-CH_2CH_2CH_2-$				0.9 ± 0.0	45.1 ± 13	50
43 (Ro 14-7527)	CH_2CH_3	$-(R)-CH_2CH_2CH_2-$				>100	>1000	

[a] Values for new compounds are listed with statistical limits and represent $\bar{X}$ ± SEM ≥ 3 experiments. [b] See ref 8 for details. [c] See ref 37 for details.

least squares fitted to the A-, B-, and C-ring atoms of **1** (Ro 15-4513) using the FIT option of SYBYL, with the exception of **3**, **44**, and **45**, in which only the B and C rings were matched to those of **1**. The steric and electrostatic potentials were generated using an sp^3 carbon probe with a +1 charge. The grid used in the CoMFA study had a resolution of 2.0 Å and the grid dimensions ran from −6.0 to +12.0 Å along the *X* axis, −8.0 to +8.0 along the *Y* axis, and from −6.0 to +8.0 along the *Z* axis. These dimensions insured that the grid extended beyond the molecular dimensions by 4.0 Å in all directions and that the *Z* coordinates of ring A (0.0 Å) matched exactly the *Z* coordinate of one plane of the potential grid. The "Minimum_sigma" value was set to 1.00. The "QSAR Empty_value", "CoMFA switching", and "PLS scaling" tailor options were set to "column_mean", "no", and "comfa_std" respectively.

Excluded Volume. Ligands which possessed BzR affinities of ≤10 nM or ≥100 nM were considered as "active" or "inactive" respectively in the excluded volume analysis. Applying these definitions to the binding data for the DI site, compounds **1**, **3**, **6**, **14**, and **16** were classified as active and compounds **7-9**, **12**, **17**, **18-23**, **34**, **35**, **40**, and **46-48** were deemed inactive. For the DS site, ligands **1-10**, **12**, **15**, **16**, **20**, **25**, **26**, **28**, **31-37**, **42**, and **44-48** were considered as active and compounds **18**, **19**, **21**, **22**, **40**, and **41** were classified as inactive. The ab initio 3-21G geometries of the ligands (see above) were used for the excluded volume analysis. The conformations of the "inactive" ligands were generated and minimized by using the MULTIC (30° torsional resolution) and MM2 BatchMin options of MacroModel version 3.5, respectively. All conformations which were within 3 kcal/mol of the global energy minimum were included in the excluded-volume analysis since presumably none of the low-energy conformations fit the receptor well. In the minimization process, all atoms except those in the flexible side chains were held fixed. The excluded receptor volume was generated by using the MVOL option of Sybyl version 5.5 by subtracting the union of the volume of "actives" from the union of volume of

Table IV. Affinity of Miscellaneous 1,4-Diazepine Derivatives for the DS and DI Benzodiazepine Receptors

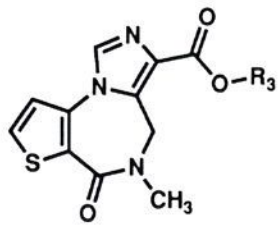

3 (Ro 19-4603)
44
45

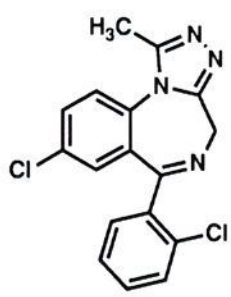

46 (Triazolam)

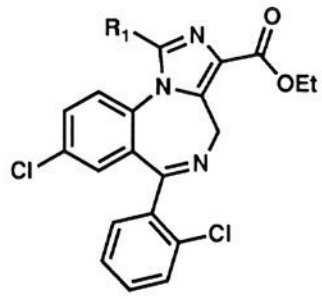

47 (Ro 21-7254)
48 (Ro 21-8303)

compound	R_1	R_3	DS (nM)[a]	DI (nM)[a]	DI/DS
3[b] (Ro 19–4603)		$C(CH_3)_3$	0.2 ± 0.0	2.6 ± 0.2	13
44[c]		CH_3	0.9 ± 0.1	51.9 ± 5.8	58
45[c]		$CH_2CH_2CH_3$	1.4 ± 0.3	38.2 ± 1.4	27
46[b] (triazolam)			0.8 ± 0.1	2086 ± 681	2608
47[b] (Ro 21–8303)	H		1.9 ± 0.1	1024 ± 178	539
48[b] (Ro 21–7254)	CH_3		2.2 ± 0.1	2810 ± 198	1277

[a] Values for new compounds are listed with statistical limits and represent $\bar{X} \pm SEM \geq 3$ experiments. [b] See ref 8 for details. [c] See ref 37 for details.

"inactives". Conversely the receptor essential volume was produced by subtracting the union of the volume of "inactives" from the union of volume of "actives".

Electrostatic Potentials. The starting geometries of ethyl formate (**50**), 3-methyl-1,2,4-oxadiazole (**51**), and 2-methyl-1,3,4-oxadiazole (**52**) (Table VIII) were constructed using version 2.91 of CONCORD. The CONCORD geometries were fully optimized using the Gaussian 90 program with the 6-31G* basis set. Electrostatic potentials were calculated directly from the 6-31G* wave function using the program MOLGRAF. A distance-based penalty function was added to the optimizer to locate minima at 1.8 Å (hydrogen-bonding distance) from the respective heteroatom.

Results and Discussion

The affinities of a series of imidazo-1,4-diazepines for the DI and DS BzR are presented in Tables I–IV. Substitution at the 7- or 8-positions appears to be required for high affinity binding to the DI BzR. Thus, analogs lacking substituents at either of these positions display relatively low affinity for the DI site [e.g., **8** (K_i = 1409 nM) and **23** (K_i = 1132 nM)].[33] In contrast, substitutions at the 9- and 10-positions are not well tolerated as evidenced by the low affinities (K_i > 10 000 nM) of the 9- and 10-chloro derivatives **21** and **22**, respectively.[34] While substituents at positions 7 and 8 enhance ligand affinity at the DI site, substitution at position 8 results in somewhat higher affinity for the DI site than does position 7 [e.g., 7-chloro-1,4-benzodiazepine **25** (K_i = 20.9 nM) vs the 8-chloro analog **24** (K_i = 10.9 nM)]. In contrast, substitution at the 7-position increases ligand affinity at DS more than substitution at position 8 [compare **25** (K_i = 0.4 nM) vs **24** (K_i = 13.7 nM)]. Hence, the net effect of substitution at the 8-position is to enhance selectivity for the DI site.

As the size of the ester group at position 3 of the imidazo[1,5-*a*][1,4]benzodiazepine ring system increases, ligand affinity at DI also increases. This is evident from the following series: methyl (**8**, K_i = 1409 nM), ethyl (**9**, K_i = 214 nM), and *tert*-butyl ester (**10**, K_i = 21.2 nM). A similar trend is seen with a chlorine substituent in the 8-position: methyl (**11**, K_i = 123 nM), ethyl (**12**, K_i = 16.9 nM), and *tert*-butyl ester (**16**, K_i = 1.7 nM). However, as the size of the alkyl group becomes larger than *tert*-butyl, affinity is diminished: $CH(CH_2CH_3)_2$ (**17**, K_i = 122.6 nM), CH_2-t-Bu (**18**, K_i = 299.6 nM), and CH_2-CH_2-t-Bu ester (**19**, K_i > 1000 nM).

Annelation of a four- or five-membered ring (ring D) on to ring B results in a slight decrease in ligand affinity at DI: no ring D (**2**, K_i = 20 nM), four-membered ring (**31**, K_i = 34 nM), and five-membered ring (**36**, K_i = 69 nM). In the same series, there is no effect on affinity at DS (K_i = 0.2 nM for all three analogs).

Replacement of the benzene A ring by thiophene results in an increase in ligand affinity at DS [compare **8** (K_i = 6.3 nM) vs **44** (K_i = 0.9 nM) and **10** (K_i = 1.1 nM) vs **3** (K_i = 0.2 nM)]. However, an even greater increase in ligand affinity for the DI site is seen with thiophene substitution [**8** (K_i = 1409 nM) vs **44** (K_i = 51.9 nM) and **10** (K_i = 21.2 nM) vs **3** (K_i = 2.6 nM)]. Hence, the net result of the A-ring thiophene replacement is enhanced selectivity for the DI site.

The qualitative SAR presented above can be summarized by examining the excluded and essential DI receptor volume maps (Figure 1). The excluded volume may be thought of as regions which are likely to be occupied by receptor in the vicinity of the bound ligand. The excluded volume map (red-colored region in Figure 1) shows forbidden regions about the 1-, 6-, 7-, 9-, and 10-positions of the imidazo[1,5-*a*][1,4]benzodiazepine ring system which correlates with the reduction in affinity for DI when large substituents are placed at any of these positions. The receptor essential volume corresponds to receptor pocket(s) which, if occupied by the ligand, enhance affinity. The receptor essential volume map (green-colored region in Figure 1) shows favorable regions in the vicinity of position 3 of the imidazo[1,5-*a*][1,4]benzodiazepine ring

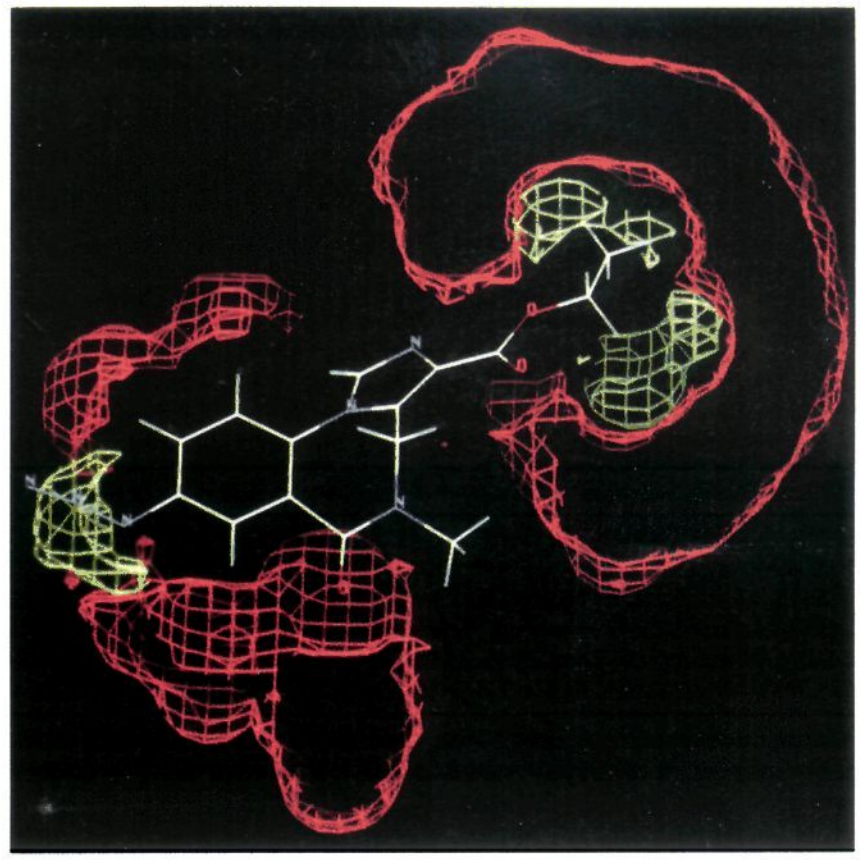

Figure 1. DI receptor essential and excluded volume maps displayed about the structure of 1 (Ro 15-4513). The essential and excluded volumes are represented by green and red wire meshes respectively and are *z*-clipped for the sake of clarity. Occupation of receptor essential (green) volume by benzodiazepine ligands is necessary for high affinity binding to the DI BzR site. Conversely, occupation of the receptor excluded (red) volume results in a decrease in affinity for the DI BzR site.

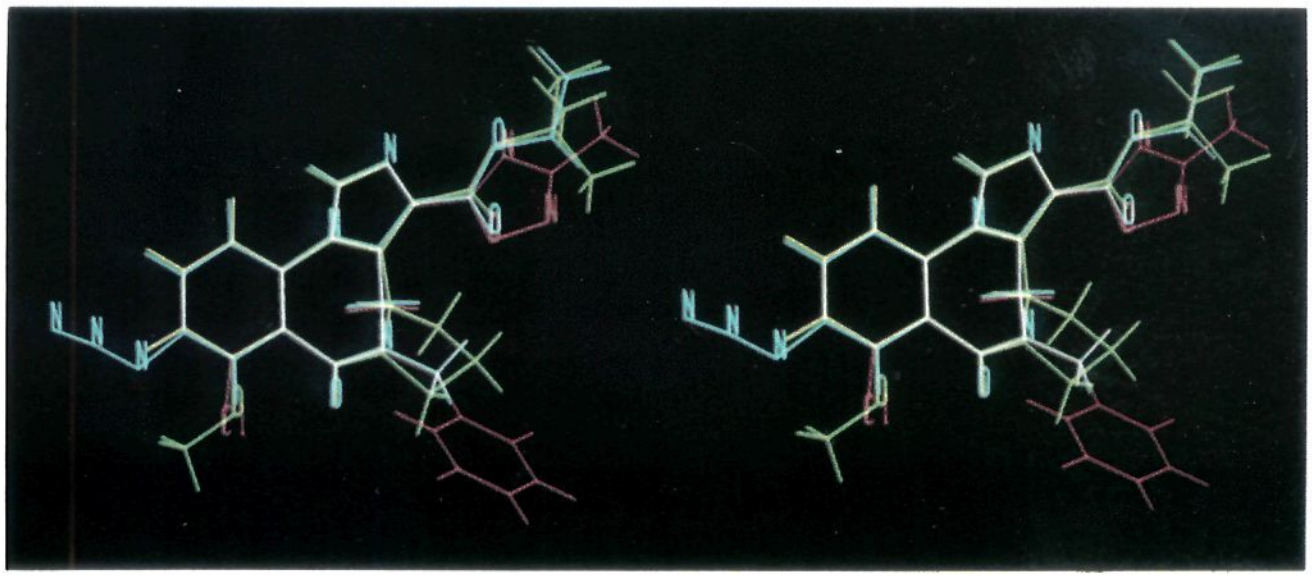

Figure 2. Stereoview of the alignment of **1** (Ro 15-4513) (blue), **26** (red), and **34** (Ro 16-3607) (green) used in the 3D-QSAR analysis.

Table V. RMS Deviations (Å) of Pairwise Least-Squares Fits between the 14 Heavy (Non-hydrogen) Atoms That Comprise the A, B, and C Rings of the X-ray Crystal Structures of Pyrrolo[2,1-*c*][1,4]benzodiazepines

X-ray crystal structure	**4**[a]	**5**[c]	**6**[c]	**42**[c,d]
4[a] (Ro 15–1788)	0.04	0.08	0.11	0.12
5[c] (Ro 17–1812)	0.08		0.10	0.14
6[c] (Ro 16–6028)	0.11	0.10		0.13
42[c,d] (Ro 14–5974)	0.12	0.14	0.13	0.07

[a] Codding, P. W.; Muir, A. K. S. Molecular structure for Ro 15–1788 and a model for the binding of benzodiazepine receptor ligands. *Mol. Pharm.* **1985**, *28*, 178–184. [b] Hempel, A.; Camerman, N.; Camerman, A. Benzodiazepine stereochemistry: crystal structures of the diazepam antagonist Ro 15–1788 and the anomalous benzodiazepine Ro 5–4864. *Can. J. Chem.* **1987**, *65*, 1608–1612. [c] This work. [d] There are two molecules per unit cell for this X-ray crystal structure.

system which correlates with the high affinity displayed by analogs which possess intermediate sized ester substituents in this position. Finally, the receptor essential volume displays a favorable region about the 8-position of the imidazo[1,5-*a*][1,4]benzodiazepine ring system, consistent with the high affinity for DI that the 8-substituted analogs possess.

The volume maps presented in Figure 1 are a qualitative description of the steric contribution to ligand binding and contain no information about possible electrostatic effects. Furthermore, volume maps cannot be used to make quantitative predictions. In order to obtain more insight into the steric and electrostatic requirements for selective, high-affinity binding to DI, a 3D-QSAR study was initiated using the CoMFA technique of Cramer et al.[18] As with all 3D-QSAR problems, the alignment rule and active conformations must first be determined. Since every analog examined in this study shares a common imidazo-1,4-diazepine substructure (see Figure 2), the alignment rule is trivial. Furthermore, good overlap is illustrated in Table V between the A, B, and C rings of the tri- and tetraheterocyclic systems available from X-ray crystallographic parameters. The determination of the active conformation is more problematic. In particular, most of the analogs examined possessed a flexible ester function at the 3-position which can adopt either a low-energy syn or anti conformation (N2—C3—C=O torsional angle = ~0 or ~180°, respectively; see Table VI). In addition, the pyrrole ring of the pyrrolo[2,1-*c*][1,4]-benzodiazepine may adopt one of two envelope conformations (see Table VII). MM2 calculations indicate that the two envelope conformations of the dione **46** differ by only 0.27 kcal/mol with the conformation available from X-ray analysis representing the higher energy conformer. Finally, **1** (Ro 15-4513) has a flexible azido substituent at position 8 which again can adopt either a syn or anti conformation (C7–C8–N–N torsional angle = ~0 or ~180°, respectively). Since **1** (Ro 15-4513) displays one of the highest affinities and selectivities for DI of any compound measured to date, it is crucial that the active conformation of this functional group be elucidated. The SAR clearly shows a preference for 7-substituents for the DS site; therefore the syn conformation of the azido functionality of **1** (Ro 15-4513) was used for the DS 3D-QSAR analysis. It was not clear, however, which conformation to employ for analysis at DI. Hence, both conformations of the azido group of **1** (Ro 15-4513) were examined for the DI study, and both the syn and anti conformations of the esters at the 3-positions were examined. Only one set of conformations yielded a satisfactory cross-validated correlation ($R^2 > 0.70$) which strongly implicates this set of conformations as being the "active" one. All other sets of conformations gave cross-validated R^2's < 0.5. The active conformation of the ester groups appears to be the same for both the DI and DS sites, and that conformation is anti. In the case of **1** (Ro 15-4513), the DI active conformation of the 8-azido group appears to be anti, in contrast to the active DS conformation which is almost certainly syn.

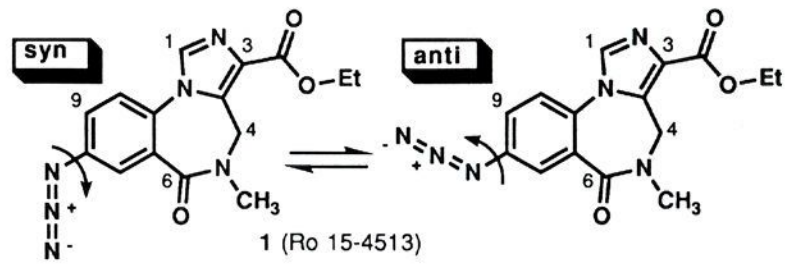

In an attempt to obtain additional evidence for the involvement of the anti conformation of the ester substituents, the magnitude of the electrostatic potential about the carbonyl and ether oxygen atoms of the esters and of the corresponding heteroatom of the oxadiazole ester bioisosteres (see Table VIII) was examined. While similar electrostatic calculations have previously been reported,[35] it was decided to replace the AM1 geometry optimizations used in the previous work with ab initio 6-31G* calculations, since semiempirical methods are known to poorly reproduce heteroatom–heteroatom bond lengths which would, in turn, adversely affect the calculations of electrostatic potential. It can be seen there is no correlation between the rank order of potency (ester ≫ 3-methyl-

Table VI. Conformations of Ester Substituents in X-ray Crystal Structures of Imidazo[1,5-*a*][1,4]benzodiazepines

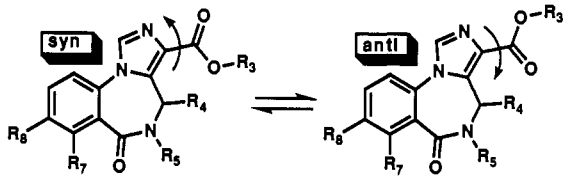

X-ray structure	R_3	R_4	R_5	R_7	R_8	N2—C3—C=O torsional angle (deg)
4[a] (Ro 15-1788)	CH_2CH_3	H	CH_3	H	F	17.1 (syn)
4[b] (Ro 15-1788)	CH_2CH_3	H	CH_3	H	F	17.3 (syn)
5[c] (Ro 17-1812)		$-CH_2CH_2-$		Cl	H	-29.0 (syn)
42[c,d] (Ro 14-5974)	CH_2CH_3	$-CH_2CH_2CH_2-$		H	H	-173.6 (anti)
42[c,d] (Ro 14-5974)	CH_2CH_3	$-CH_2CH_2CH_2-$		H	H	-152.0 (anti)
6[c] (Ro 16-6028)	$C(CH_3)_3$	$-CH_2CH_2CH_2-$		Br	H	-44.2 (syn)

[a] Codding, P. W.; Muir, A. K. S. Molecular structure for Ro 15-1788 and a model for the binding of benzodiazepine receptor ligands. *Mol. Pharm.* **1985**, *28*, 178-184. [b] Hempel, A.; Camerman, N.; Camerman, A. Benzodiazepine stereochemistry: crystal structures of the diazepam antagonist Ro 15-1788 and the anomalous benzodiazepine Ro 5-4864. *Can. J. Chem.* **1987**, *65*, 1608-1612. [c] This work. [d] There are two molecules per unit cell for this X-ray crystal structure.

Table VII. Conformation of the Pyrrole Ring in X-ray Crystallographic Structures of Pyrrolo[2,1-c][1,4]benzodiazepines

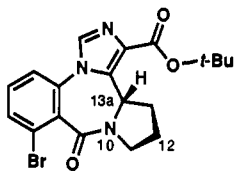

6 (Ro 16-6028)

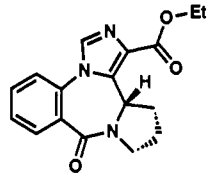

42 (Ro 14-5974)

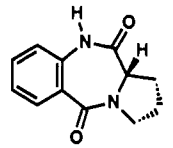

49
{(11aS)-1,2,3,10,11,11a-Hexahydro-5H-pyrrolo[2,1-c][1,4]benzodiazepine-5,11-dione}

X-ray structure	torsional angle (deg) 10-11-12-13	11-12-13-13a	12-13-13a-10	13-13a-10-11	13a-10-11-12
6[a] (Ro 16-6028)	-38.5	39.5	-24.1	-0.1	24.3
42[a,b] (Ro 14-5974)	20.1	-26.0	21.0	-9.7	-5.2
42[a,b] (Ro 14-5974)	27.6	-34.8	27.3	-9.7	-11.0
49[c]	34.4	-39.5	28.8	-7.3	-17.0

[a] This work. [b] There are two molecules per unit cell for this X-ray crystal structure. [c] Neidle, S.; Webster, G. D.; Jones, G. B.; Thurston, D. E. Structures of two DNA minor-groove binders, based on pyrrolo[2,1-c][1,4]-benzodiazepines. *Acta Crystallogr.* **1991**, *C47*, 2678-2680.

Table VIII. Affinity of 5,6-Dihydro-5-alkyl-6-oxo-4*H*-imidazo[1,5-*a*][1,4]benzodiazepine-3-carboxylate (28) and Oxadiazole Bioisosteres (29 and 30) for the DS and DI Benzodiazepine Receptors vs Magnitude and Location (Cartesian *X*-*Y* Coordinates) of 6-31G*//6-31G*// MOLGRAF Electrostatic Potential Minima about Corresponding Model Compounds (50, 51, and 52)[a]

compound			model compound		LP1			LP2			LP3		
no.	DS (nM)	DI (nM)	no.	structure	energy (kcal/mol)	*x*,*y* (Å)		energy (kcal/mol)	*x*,*y* (Å)		energy (kcal/mol)	*x*,*y* (Å)	
28	1.5	122	50	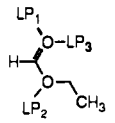	-54.27 -37.45	1.40 1.70	2.15 2.76	-31.46 -17.76	0.81 0.46	-2.15 -2.67	-50.12 —[b]	2.95 —[b]	-1.26 —[b]
29	907	>10000	51	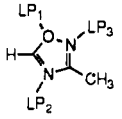	-28.38 —[b]	1.34 —[b]	2.44 —[b]	-55.27 -36.79	1.57 1.43	-2.23 -2.73	-55.15 -39.57	3.80 4.04	1.90 2.35
30	1209	>10000	52	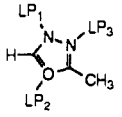	-65.47 -47.90	1.69 1.79	2.24 2.76	-15.76 -7.35	1.18 0.95	-2.37 -2.80	-66.50 -48.08	4.13 4.42	1.22 1.68

[a] The coordinate system is based upon placing the formate hydrogen atom at the origin, the carbonyl carbon atom along the *X* axis, and rotating about the H-C bond so that the C=O bond is in the *X*-*Y* plane and in the positive *Y* direction. The minima are represented schematically in the structures as LP_1-LP_3 (lone pair of electrons 1-3). For each lone pair, two minima are listed. The first corresponds to the local minima while the second is the minima located at a distance 1.8 Å from the respective heteroatom (the length of an average hydrogen bond). [b] No minima in the potential found 1.8-Å distant from this heteroatom.

1,2,4-oxadiazole > 5-methyl-1,3,4-oxadiazole) and the magnitude of the electrostatic potential about LP1, LP2, or LP3 (Table VIII). Furthermore, there is no obvious relationship between the rank order of potency vs the relative positions of the terminal methyl groups of the ethyl ester, 5-methyl-1,3,4-oxadiazole, and 3-methyl-1,2,4-

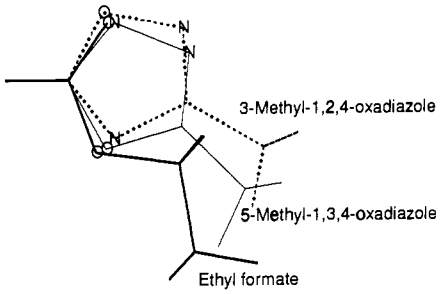

Figure 3. Overlay of ab initio 6-31G* optimized structures of ethyl formate (thick line) and the bioisosteric 5-methyl-1,3,4-oxadiazole (thin line) and 3-methyl-1,2,4-oxadiazole (dashed line).

oxadiazole substituents when overlaid (see Figure 3). Hence, the rank order of potency for these analogs is probably a result of combined steric and electrostatic effects. Only techniques such as 3D-QSAR which consider both effects simultaneously are therefore likely to provide an explanation for the relative potency of these ester bioisosters.

The final CoMFA statistics are presented in Table IX and show that good correlations were obtained for the negative logarithms of affinities at the diazepam-insensitive and -sensitive BzR sites [pK_i(DI) and pK_i(DS), respectively], and for the differences in their negative logarithms [pK_i(DI) – pK_i(DS)], the latter quantity being a measure of receptor selectivity. The steric and electrostatic contour maps derived from these correlations are presented in Figures 4–9.

In the steric CoMFA map of the DI site (see Figure 4), there are regions which are predicted to enhance affinity in the vicinity of position 8 and about the carboxylic ester attached to position 3. There is a site of negative steric interaction just beyond the favorable position 3 region which is consistent with the diminished activity of the longer ester substituents. Finally, there are areas about the 4-, 5-, and 7-positions which are predicted to diminish affinity for the DI site.

In the DI electrostatic map (see Figure 5), there is an area in the plane of and located below the ester carbonyl oxygen atom (corresponding roughly to LP3 in Table VIII), whereby increases in the negative electrostatic potentials is predicted to decrease affinity. This is probably a consequence of the relatively low affinities displayed by the oxadiazole derivatives **26**, **27**, and **30** relative to their ester congeners **25**, **24**, and **30**, respectively. Note that the electrostatic potential about LP3 is lower for the oxadiazoles **51** and **52** than for the ethyl ester **50**. There is also a region about the 8-position wherein increases in negative electrostatic potential are predicted to increase affinity, while there are areas in the vicinity of the 9-position wherein increases in negative electrostatic potential are predicted to decrease affinity. These contours are probably a consequence of the relatively high affinity displayed by electronegative chlorine substituents in the 8-position and the correspondingly low affinities by the 9- and 10-chloro analogs. This latter feature of the electrostatic map may be an artifact since all of the 9- and 10-substituted derivatives have a chlorine substituent which carries a partial negative charge. This effect may therefore be steric rather than electrostatic.[34]

The steric DS CoMFA map (Figure 6) illustrates unfavorable steric regions in the vicinity of the 8-position and a favorable region about the 7-position and the alkyl groups of the carboxylic ester at the 3-position. There is an area of negative steric interaction just beyond the favorable steric regions about position 3, similar to what is seen in the steric DI map. In addition, there is a negative steric region about the ortho position and a positive region about the para position of the 5-benzyl derivatives. This is not surprising, since the benzyl analogs displayed relatively low affinities compared to their methyl congeners: **25** (K_i = 0.4 nM) vs **2** (K_i = 0.2 nM) and **24** (K_i = 13.7 nM) vs **12** (K_i = 5.4 nM), while the allyl derivative displays much lower affinity: **23** (K_i = 39.2 nM) vs **9** (K_i = 1.3 nM).

The electrostatic DS CoMFA map (Figure 7) shows contours in the vicinity of the 8-position in which increases in negative electrostatic potential are predicted to decrease affinity while there are regions above and below the plane of the aromatic carbons at the 8- and 9-positions in which increases in positive electrostatic potential are predicted to enhance affinity. These contours are likely a result of the relatively low affinity displayed by electronegative chlorine substituents at the 8- and 9-positions. The electrostatic maps for both DI and DS receptor sites closely resemble each other about position-3. Since the oxadiazoles **26**, **27**, and **30** uniformly display lower affinity than their ester analogs for the DS as well as the DI site, the arguments presented above for this portion of the DI electrostatic CoMFA map also apply to the DS electrostatic map.

In the DI/DS steric CoMFA map (Figure 8), substituents which occupy the region of space between the 8- and 9-positions [e.g., the anti azido conformer of **1** (Ro 15-4513)] are predicted to enhance ligand selectivity at DI while substituents that occupy position 7 are predicted to decrease selectivity. There are also weaker selectivity enhancing contours for DI about the alkyl groups of the 3-ester group. The electrostatic DI/DS CoMFA map (Figure 9) contains a region between the 7- and 8-substituents which suggests that DI selectivity should be enhanced if electrostatic potential is made more negative. There are also areas above the 7-position and between the 8- and 9-positions where DI selectivity should be enhanced by increases in positive electrostatic potential.

We have previously demonstrated that CoMFA is capable of making quantitatively useful predictions of binding affinity for a series of 3-substituted β-carbolines at the DS site.[36] Efforts are currently underway to use CoMFA regression equations and maps derived in this work in the design of more potent and selective ligands for the DI site.

Experimental Section

Materials. [^{3}H]Ro 15-4513 was purchased from DuPont-NEN (Boston, MA). Diazepam and compounds with an 'Ro' prefix were donated by Hoffmann-La Roche of Nutley, NJ, and of Basel, Switzerland. Triazolam was a gift of K. H. Weber. Compounds **7**, **8**, **10**, **11**, and **13-19** (Table I) and compounds **44** and **45** (Table IV) were prepared by acid hydrolysis of the Hoffmann-La Roche derivatives **2** (Ro 15-3505), **3** (Ro 19-4603), **5** (Ro 15-1788), or **9** (Ro 14-7437), followed by acid chloride formation and condensation with the corresponding alcohol.[37] The analogs from Table II (**23-30**) were prepared according to the procedure of Ananthan et al.[38]

Receptor Binding. [^{3}H]Ro 15-4513 binding to DI and DS benzodiazepine receptor in rat cerebellum was determined as previously described.[8] In brief, cerebella from adult, male Sprague–Dawley rats were dissected, weighed, and disrupted (Brinkmann Polytron, setting 6, 10s) in 60 volumes of 50 mM Tris-citrate buffer (pH = 7.8). Homogenates were centrifuged

Table IX. CoMFA Statistics for K_i Data at the DS and DI Sites for 38 BzR Ligands

dependent variable	number of cross validation groups	optimal number of components	r^2	F value	standard error estimate	probability $r^2 = 0$	relative contributions	
							steric[c]	electrostatic[d]
pDI[a]	38	7	0.73	7.199	0.451	0.000	0.642 ± 0.008	0.358 ± 0.008
pDI[a]	0	7	0.96	97.459	0.177	0.000	0.650	0.350
pDS[b]	38	11	0.70	4.952	0.588	0.000	0.640 ± 0.010	0.360 ± 0.010
pDS[b]	0	11	0.99	323.263	0.092	0.000	0.650	0.350
pDI – pDS	38	6	0.79	7.746	0.556	0.000	0.670 ± 0.007	0.330 ± 0.007
pDI – pDS	0	6	0.98	221.233	0.182	0.000	0.695	0.305

[a] pDI = $-\log(K_i)$ diazepam insensitive BzR binding. [b] pDS = $-\log(K_i)$ diazepam sensitive BzR binding. [c] Combined contribution of 139 steric potentials (selected by setting minimum $\sigma = 1.0$) out of a possible $8 \times 9 \times 10 = 720$ potentials. [d] Combined contribution of 139 out of a possible 720 electrostatic potentials.

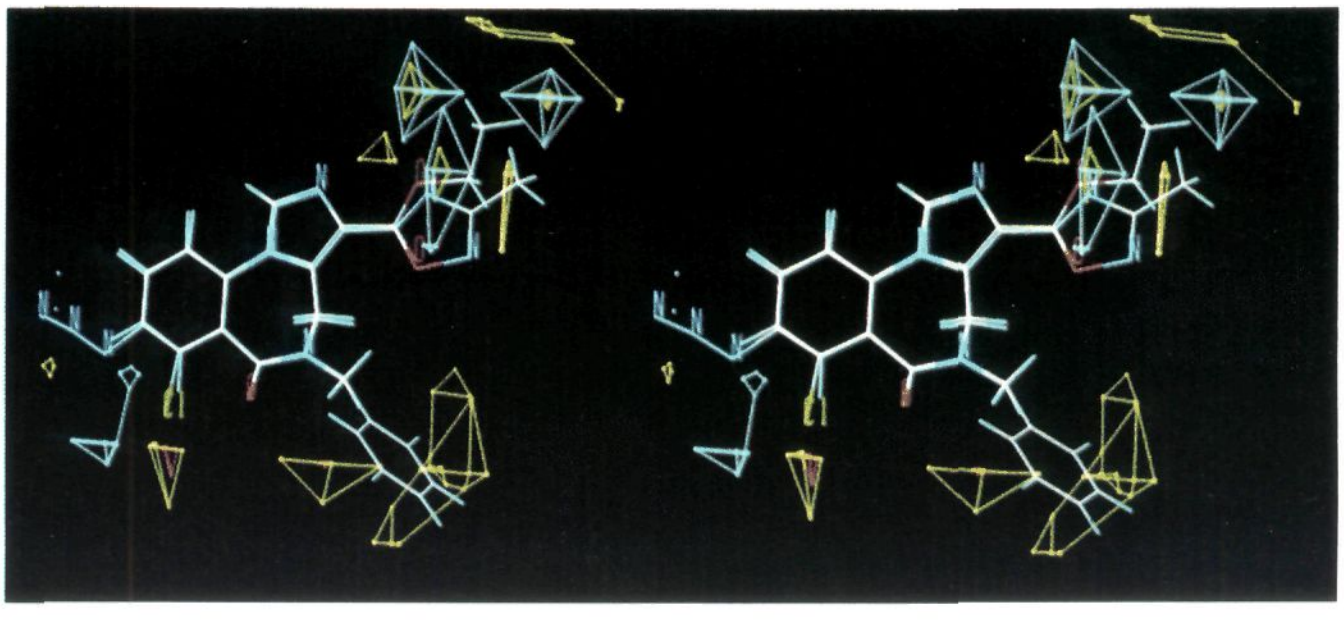

Figure 4. Stereoview of DI steric CoMFA map. Green and cyan contours surround regions where a higher steric interaction is predicted to increase affinity (the QSAR coefficients times the standard deviation of the corresponding column are greater than +0.10 and +0.05, respectively). Yellow and red contours surround regions where a lower steric interaction is predicted to increase affinity (less than −0.03 and −0.06, respectively). Molecules displayed are **1** (Ro 15-4513) and **26**.

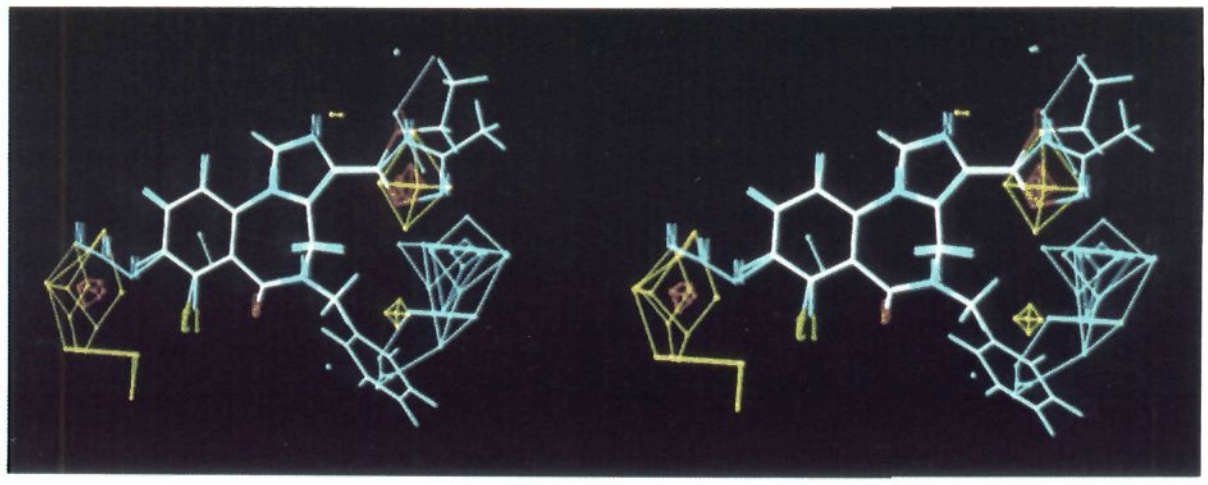

Figure 5. Stereoview of DI electrostatic CoMFA map. Red and yellow contours surround regions where a more negative electrostatic interaction is predicted to increase affinity (the QSAR coefficients times the standard deviation of the corresponding column are less than −0.04 and −0.02, respectively). Cyan and blue contours surround regions where a positive electrostatic interaction is predicted to increase affinity (greater than +0.02 and +0.04, respectively). Molecules displayed are the same as in Figure 4.

at 20000*g* for 20 min (4 °C), resuspended in 60 volumes of buffer, and recentrifuged. This centrifugation procedure was repeated five times. Membranes were reconstituted in 50 volumes of buffer and used immediately in the binding assay. Radioligand binding to DS + DI benzodiazepine receptors was determined in a solution consisting of: tissue (~100 μg), [^{3}H]Ro 15-4513 (sp. act. 24.3 Ci/mmol, New England Nuclear, final concentration ~2 nM), 0.2 M NaCl, 50 μL competitor to a total volume of 0.5 mL with Tris-citrate buffer (pH = 7.8). Radioligand binding to DI was determined exactly as described above except that 10 μM diazepam was also added to the solution; binding to DS was the difference between values obtained for ligand binding to DI and DS + DI benzodiazepine receptor. Nonspecific binding was determined in the presence of 10 μM 4 (Ro 15-1788) and was typically <10% and <20% of total binding for DS and DI, respectively. Assays were performed in duplicate. Values are the mean ± standard error unless otherwise indicated. Incubations (0–4 °C) were terminated after 60 min by rapid filtration through Whatman GF/B filters with a Brandel (M48-R) manifold followed by two 5-mL washes with ice-cold buffer. The radioactivity retained on the filter was measured by scintillation counting. IC_{50} values were generated using at least six concentrations of compound with an iterative curve fitting program (Graph Pad, Inplot 3.15).

X-ray Analysis of 5 (Ro 17-1812). A colorless prismatic crystal with approximate dimensions of 0.17 × 0.25 × 0.45 mm was selected for data collection. The crystal belongs to the orthorhombic space group $P2_1P2_1P2_1$ with a = 7.545(3) Å, b = 8.392(3) Å, c = 25.878(9) Å, $\alpha = \beta = \gamma = 90°$, and $Z = 4$. The molecular formula is $C_{18}H_{16}ClN_3O_3$ (formula weight = 357.79), and the calculated density is 1.45 g/cm^3. A Nicolet P3m diffractometer was used to collect 1934 independent reflections with $F > 2.5\sigma(F)$ at a temperature of 183 K with monochromated

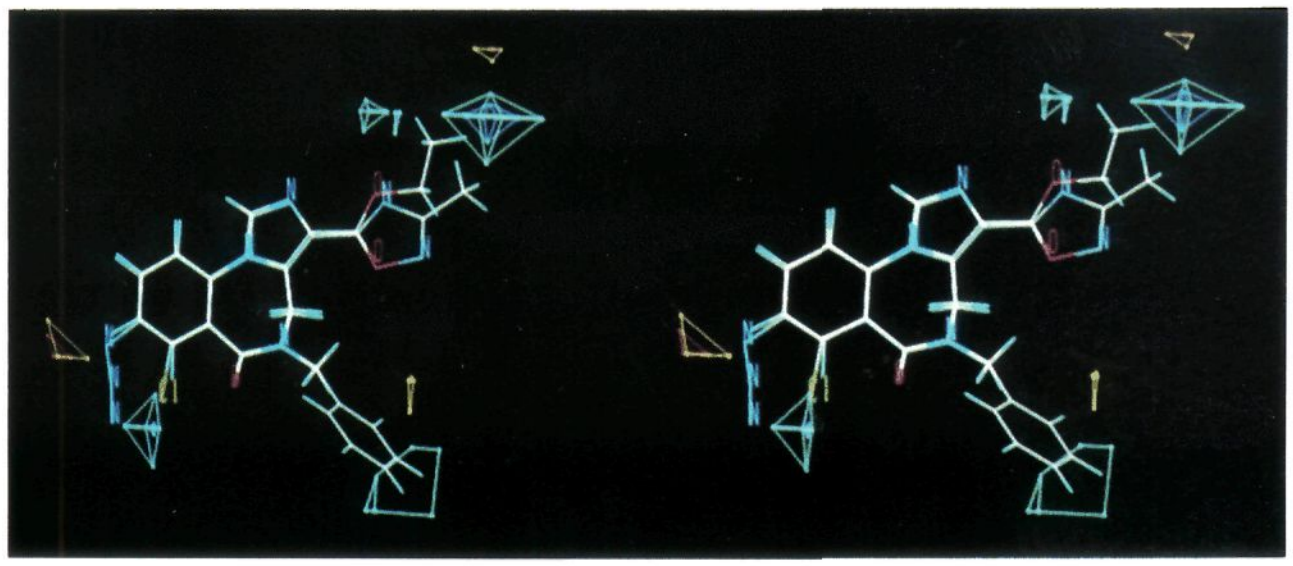

Figure 6. Stereoview of DS steric CoMFA map. Green and cyan contours surround regions where a higher steric interaction is predicted to increase affinity (the QSAR coefficients times the standard deviation of the corresponding column are greater than +0.10 and +0.05, respectively). Yellow and red contours surround regions where a lower steric interaction is predicted to increase affinity (less than −0.10 and −0.15, respectively). Molecules displayed are the same as in Figure 4.

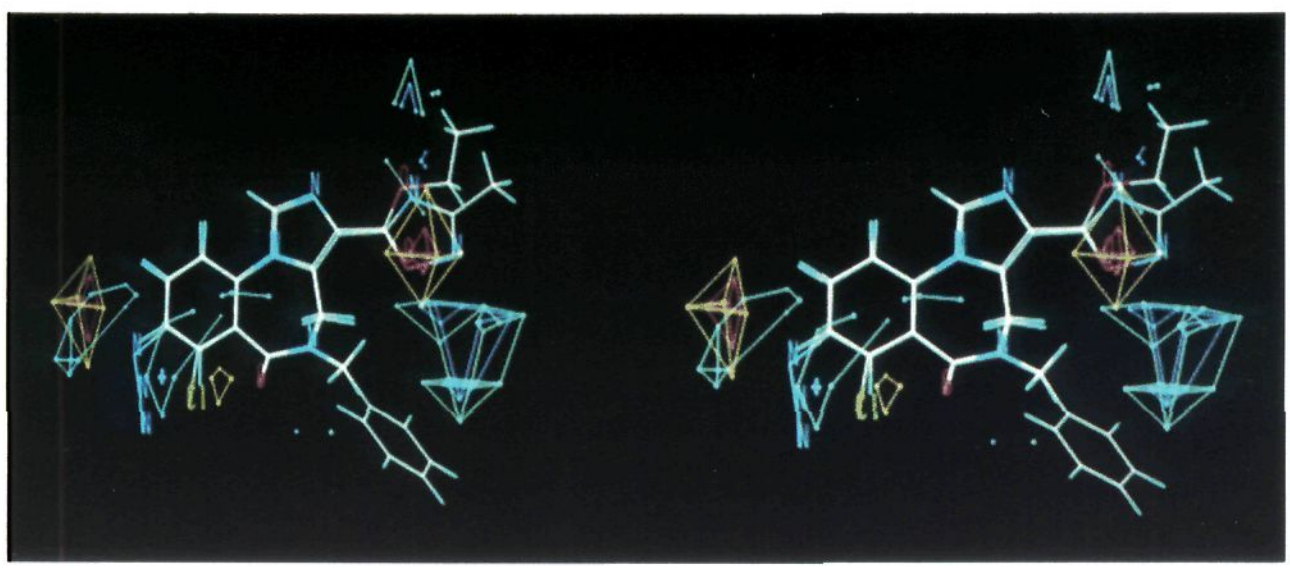

Figure 7. Stereoview of DS electrostatic CoMFA map. Red and yellow contours surround regions where a more negative electrostatic interaction is predicted to increase affinity (the QSAR coefficients times the standard deviation of the corresponding column are less than −0.10 and −0.05, respectively). Cyan and blue contours surround regions where a positive electrostatic interaction is predicted to increase affinity (greater than +0.02 and +0.04, respectively). Molecules displayed are the same as in Figure 4.

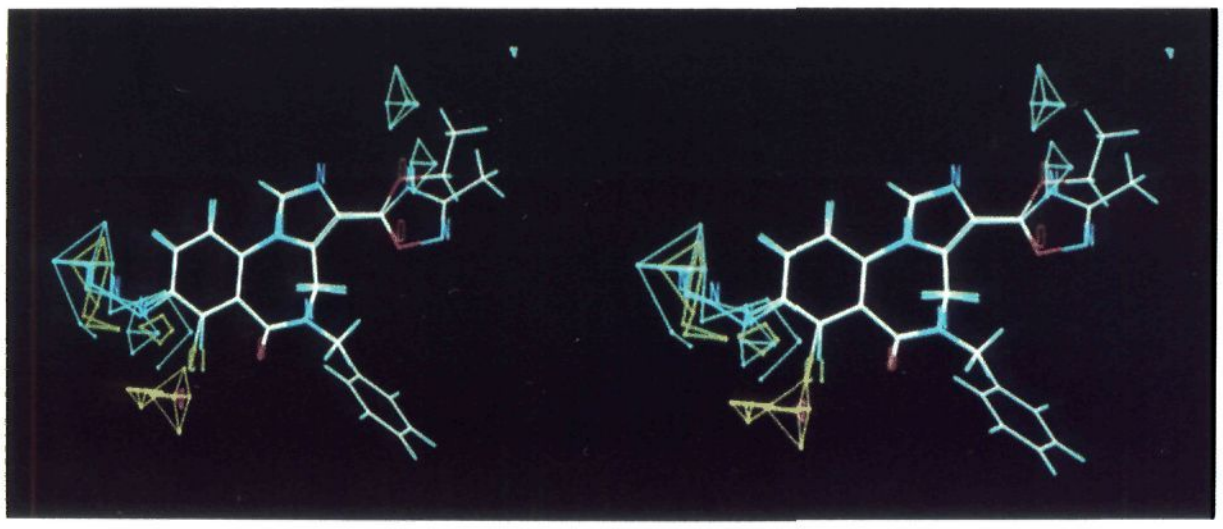

Figure 8. Stereoview of pDI − pDS steric CoMFA map. Green and cyan contours surround regions where a higher steric interaction is predicted to increase selectivity for DI (the QSAR coefficients times the standard deviation of the corresponding column are greater than +0.10 and +0.05, respectively). Yellow and red contours surround regions where a greater steric interaction is predicted to decrease selectivity for DI (less than −0.06 and −0.10, respectively). Molecules displayed are the same as in Figure 4.

Mo Kα radiation (λ = 0.710 69 Å). The structure was solved using direct methods using the Nicolet SHELXTL software.[39] The number of parameters used was 370 and yielded a final R index of 4.04.

X-ray Analysis of 6 (Ro 16-6028). A colorless prismatic crystal with approximate dimensions of 0.17 × 0.17 × 0.5 mm was selected for data collection. The crystal belongs to the orthorhombic space group $P2_1P2_1P2_1$ with a = 9.299(2) Å, b = 9.584(2) Å, c = 19.736(8) Å, $\alpha = \beta = \gamma = 90°$, and Z = 4. The molecular formula is $C_{19}H_{20}BrN_3O_3$ (formula weight = 418.29), and the calculated density is 1.58 g/cm^3. A Nicolet P3m diffractometer was used to collect 2416 independent reflections with $F > 2.5\sigma(F)$ at a temperature of 183 K with monochromated Mo Kα radiation (λ = 0.710 69 Å). The structure was solved using direct methods using the Nicolet SHELXTL software.[39] The number of parameters used was 239 and yielded a final R index of 4.26.

X-ray Analysis of 42 (Ro 14-5974). A colorless prismatic crystal with approximate dimensions of 0.35 × 0.35 × 0.45 mm was selected for data collection. The crystal belongs to the orthorhombic space group $P2_1P2_1P2_1$ with a = 13.964(4) Å, b = 7.702(3) Å, c = 33.776(12) Å, $\alpha = \beta = \gamma = 90°$, and Z = 8. The

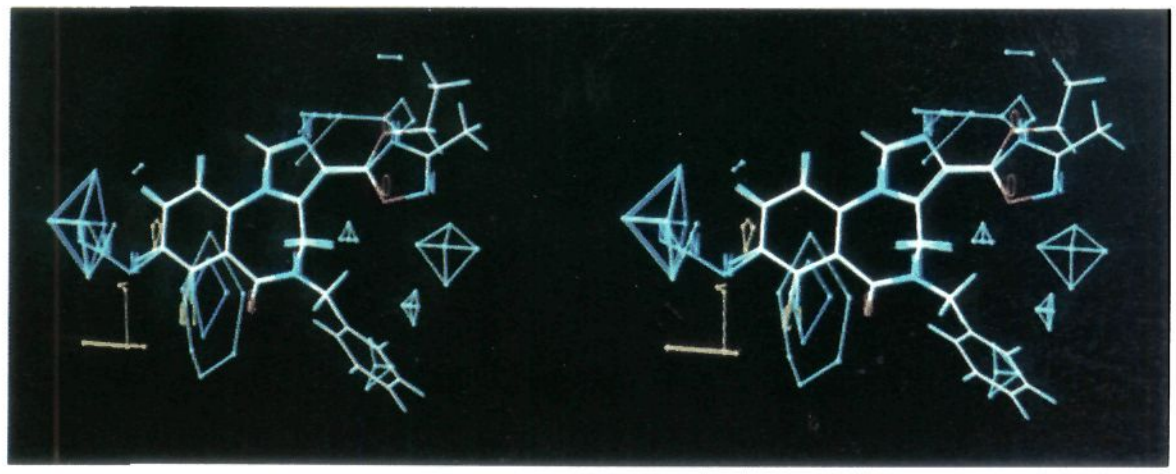

Figure 9. Stereoview of pDI – pDS electrostatic CoMFA map. Red and yellow contours surround regions where a more negative electrostatic interaction is predicted to increase selectivity for DI (the QSAR coefficients times the standard deviation of the corresponding column are less than –0.06 and –0.03, respectively). Cyan and blue contours surround regions where a positive electrostatic interaction is predicted to enhance selectivity for DI (greater than +0.012 and +0.024, respectively). Molecules displayed are the same as in Figure 4.

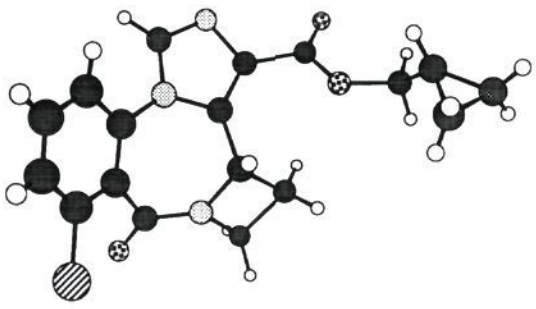

Figure 10. A perspective drawing of the X-ray determined structure of **5** (Ro 17-1812).

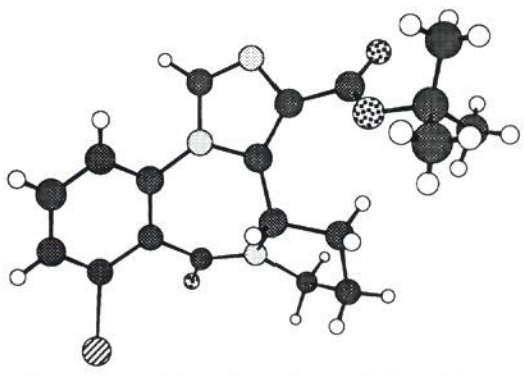

Figure 11. A perspective drawing of the X-ray determined structure of **6** (Ro 16-6028).

molecular formula is $C_{17}H_{17}N_3O_3$ (formula weight = 281.34), and the calculated density is 1.03 g/cm^3. A Hilger & Watts/PDP8 diffractometer was used to collect 2834 independent reflections at a temperature of 298 K with monochromated Cu Kα radiation (λ = 1.541 78 Å). The structure was solved using direct methods using software developed by F. R. Ahmed.[40] The number of parameters used was 208 and yielded a final R index of 10.3. There is some electron density in the final difference Fourier map which cannot be identified as solvent.

Acknowledgment. We would like to thank T. J. O'Donnell and Dale Spangler for making available to us their ESPFIT and MOLGRAF programs, respectively. We would also like to thank Peter Sorter for generous donation of compounds.

Supplementary Material Available: Tables of atomic positional and thermal parameters, anisotropic thermal parameters for nonhydrogen atoms, bond distances, and bond angles for **5** (Ro 17-1812), **6** (Ro 16-6028), and **42** (Ro 14-5974), predicted binding affinities for the DI and DS sites (pDI, pDS, and pDI – pDS) and standard error estimates (PRESS) for each of the components in the pDI, pDS, and pDI – pDS correlations, and ab initio optimized coordinates, connection tables, and ESPFIT atomic charges for the 38 molecules in the CoMFA training set and the three molecules (**50-52**) listed in Table VIII (37 pages). Ordering information given on any current masthead page.

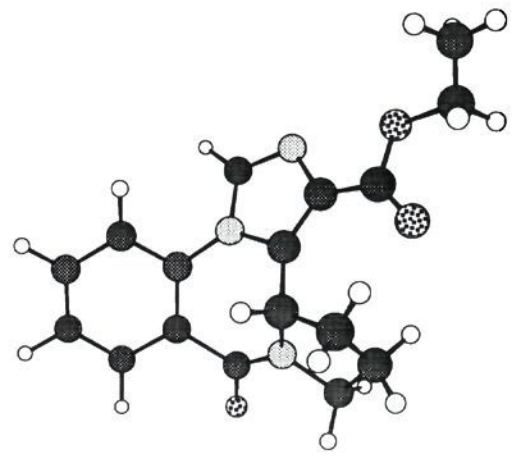

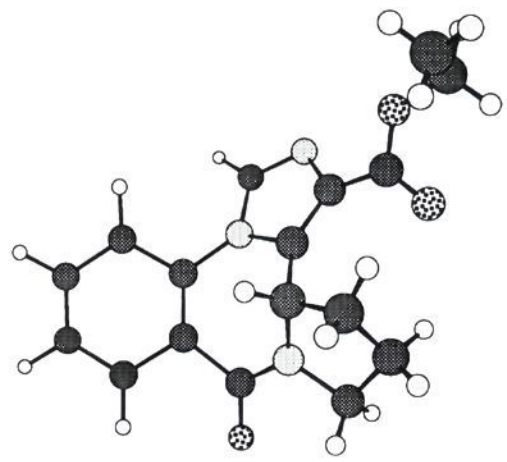

Figure 12. A perspective drawings of the two molecules in the unit cell in the X-ray determined structure of **42** (Ro 14-5974).

References

(1) *GABA and Benzodiazepine Receptors*; Squires, R., Ed.; CRC Press: Boca Raton, Florida, 1988; Vols. 1–2.
(2) Wong, G.; Sei, Y.; Skolnick, P. Stable expression of type I γ-aminobutyric acid$_A$/benzodiazepine receptors in a transfected cell line. *Mol. Pharm.* **1992**, *42*, 996–1005.
(3) Skolnick, P.; Wong, G. Drug-receptor interactions in anxiety. In *Imidazopyridines in Anxiety Disorders: A Novel Experimental and Therapeutic Approach*; Zivkovic, B., Langer, S., Bartholini, G., Ed.; Raven Press: New York, New York, 1993; pp 23–32.
(4) Olsen, R. W.; Tobin, A. J. Molecular biology of GABA$_A$ receptors. *FASEB J.* **1990**, *4*, 1469–80.
(5) Malminiemi, O.; Korpi, E. R. Diazepam-insensitive [^{3}H]-Ro 15-4513 binding in intact cultured cerebellar granule cells. *Eur. J. Pharmacol.* **1989**, *169*, 53–60.
(6) Uusi-Oukari, M.; Korpi, E. R. Diazepam sensitivity of the binding of an imidazobenzodiazepine, [^{3}H]Ro 15-4513, in cerebellar membranes from two rat lines developed for high and low alcohol sensitivity. *J. Neurochem.* **1990**, *54*, 1980–7.
(7) Turner, D. M.; Sapp, D. W.; Olsen, R. W. The benzodiazepine/alcohol antagonist Ro 15-4513: binding to a GABA$_A$ receptor subtype that is insensitive to diazepam. *J. Pharmacol. Exp. Ther.* **1991**, *247*, 1236–42.

(8) Wong, G.; Skolnick, P. High affinity ligands for 'diazepam-insensitive' benzodiazepine receptors. *Eur. J. Pharm. Mol. Pharm. Sec.* **1992**, *225*, 63–68.
(9) Wong, G.; Skolnick, P.; Katz, J.; Witkin, J. Transduction of a discriminative stimulus through a diazepam-insensitive $GABA_A$ receptor. *J. Pharmacol. Ex. Ther.*, in press.
(10) Korpi, E. R.; Uusi-Oukari, M.; Wegeluis, K. Substrate specificity of diazepam-insensitive cerebellar [^{3}H]Ro 15-4513 binding sites. *Eur. J. Pharm.* **1992**, *213*, 323–329.
(11) Luddens, H.; Pritchett, D. B.; Kohler, M.; Killisch, I.; Keinanen, K.; Monyer, H.; Sprengel, R.; Seeburg, P. H. Cerebellar $GABA_A$ receptor selective for a behavioural alcohol antagonist. *Nature* **1990**, *346*, 648–51.
(12) Luddens, H.; Wisden, W. Function and pharmacology of multiple $GABA_A$ receptor subunits. *Trends Pharmacol. Sci.* **1991**, *12*, 49–51.
(13) Lister, R. G. Antagonism of the behavioral effects of ethanol, sodium pentobarbital, and Ro 15-4513 by the imidazodiazepine Ro 15-3505. *Neurosci. Res. Commun.* **1988**, *2*, 85–92.
(14) Lister, R. G.; Durcan, M. J. Antagonism of the intoxicating effects of ethanol by the potent benzodiazepine receptor ligand Ro 19-4603. *Brain Res.* **1989**, *482*, 141–144.
(15) Harris, C. M.; Lal, H. Central nervous system effects of the imidazobenzodiazepine Ro 15-4513. *Drug Dev. Res.* **1988**, *13*, 187–203.
(16) Marshall, G. R.; Barry, C. D.; Bosshard, H. E.; Dammkoehler, R. A.; Dunn, D. A. The conformational parameter in drug design: the active analog approach. In *Computer-Assisted Drug Design*; *ACS Symposium Series 112*; Olson, E. C., Christoffersen, R. E., Ed.; American Chemical Society: Washington, DC, 1979; Vol. 112; pp 205–226.
(17) Sufrin, J. R.; Dunn, D. A.; Marshall, G. R. Steric mapping of the L-methionine binding site of ATP: L-methionine S-adenosyltransferase. *Mol. Pharm.* **1981**, *19*, 307–313.
(18) Cramer, R. D.; Patterson, D. E.; Bunce, J. D. Comparative Molecular Field Analysis (CoMFA). 1. Effect of Shape on Binding of Steroids to Carrier Proteins. *J. Am. Chem. Soc.* **1988**, *110*, 5959–5967.
(19) CONCORD; Pearlman, R. S.; Balducci, R.; McGarity, C.; Rusinko, A., III; Skell, J.; University of Texas, Austin, TX, 1990.
(20) Available from Daylight Chemical Information Systems, Inc., Irvine, CA 92714.
(21) Available from Tripos Associates, Inc., St. Louis, MO 63144.
(22) Spangler, D. P. Unpublished results. MOLGRAF has been shown to reproduce Gaussian 90 electrostatic potentials.
(23) O'Donnell, T. J.; Spangler, D. P. Unpublished results.
(24) Gaussian 90; Frisch, M. J.; Head-Gordon, M.; Trucks, G. W.; Foresman, J. B.; Schlegel, H. B.; Raghavachari, K.; Robb, M. A.; Binkley, J. S.; Gonzalez, C.; Defrees, D. J.; Fox, D. J.; Whiteside, R. A.; Seeger, R.; Melius, C. F.; Baker, J.; Martin, L. R.; Kahn, L. R.; Stewart, J. J. P.; Topiol, S.; Pople, J. A.; Gaussian, Inc., Pittsburgh, PA, 1990.
(25) Gaussian 92, Revision A; Frisch, M. J.; Trucks, G. W.; Head-Gordon, M.; Gill, P. M. W.; Wong, M. W.; Foresman, J. B.; Johnson, B. G.; Schlegel, H. B.; Robb, M. A.; Replogle, E. S.; Gomperts, R.; Anderes, J. L.; Raghavachari, K.; Binkley, J. S.; Gonzalez, C.; Martin, L. R.; Fox, D. J.; Defrees, D. J.; Baker, J.; Stewart, J. J. P.; Pople, J. A.; Gaussian, Inc., Pittsburgh, PA, 1992.
(26) Mohamadi, F.; Richards, N. G. J.; Guida, W. C.; Liskamp, R.; Caufield, C.; Chang, G.; Hendrickson, T.; Still, W. C. MacroModel-An integrated software system for modeling organic and bioorganic molecules using molecular mechanics. *J. Comput. Chem.* **1990**, *11*, 440–467.
(27) Available from the Department of Chemistry, Columbia University, New York, NY 10027.
(28) Codding, P. W.; Muir, A. K. S. Molecular structure of Ro 15-1788 and a model for the binding of benzodiazepine receptor ligands. *Mol. Pharm.* **1985**, *28*, 178–184.
(29) Hempel, A.; Camerman, N.; Camerman, A. Benzodiazepine stereochemistry: crystal structures of the diazepam antagonist Ro 15-1788 and the anomalous benzodiazepine Ro 5-4864. *Can. J. Chem.* **1987**, *65*, 1608–1612.
(30) Neidle, S.; Webster, G. D.; Jones, G. B.; Thurston, D. E. Structures of two DNA minor-groove binders, based on pyrrolo[2,1-c][1,4]-benzodiazepines. *Acta Crystallogr.* **1991**, *C47*, 2678–2680.
(31) Allinger, N. L. Conformational analysis. 130. MM2. A hydrocarbon force field utilizing V_1 and V_2 torsional terms. *J. Am. Chem. Soc.* **1977**, *99*, 8127–8134.
(32) Besler, B. H.; Merz, J. K. M.; Kollman, P. A. Atomic charges derived from semiempirical methods. *J. Compt. Chem.* **1989**, *11*, 431–439.
(33) Exceptions to this rule are derivatives **10** (K_i = 21.2 nM) and **42** (K_i = 45.1 nM) in which the optimal C-ring *tert*-butyl ester functional group (for DI binding, vide infra) and the less optimal ethyl ester respectively are able to partially compensate for the absence of A-ring substituents. Finally, derivative **3** (K_i = 2.6 nM), which contains both the optimal *tert*-butyl C-ring ester substituent and a favorable thiophene A ring (vide infra) together fully compensate for the lack of A-ring substituents.
(34) This is a preliminary conclusion based on the binding data of only two compounds. The exploration of this region of the DI receptor with additional analogs is underway and will be reported in due course.
(35) Orlek, B. S.; Blaney, F. E.; Brown, F.; Clark, M. S. G.; Hadley, M. S.; Hatcher, J.; Riley, G. J.; Rosenberg, H. E.; Wadsworth, H. J.; Wyman, P. Comparison of azabicyclic esters and oxadiazoles as ligands for the muscarinic receptor. *J. Med. Chem.* **1991**, *34*, 2726–2735.
(36) Allen, M. S.; La Loggia, A. J.; Dorn, L. J.; Martin, M. J.; Costantino, G.; Hagen, T. J.; Koehler, K. F.; Skolnick, P.; Cook, J. M. Predictive binding of β-carboline inverse agonists and antagonists via the CoMFA/GOLPE approach. *J. Med. Chem.* **1992**, *35*, 4001–4010.
(37) Gu, Z.-Q.; Wong, G.; Dominguez, C.; de Costa, B. R.; Rice, K. C.; Skolnick, P. Synthesis and evaluation of imidazo[1,5-a][1,4]-benzodiazepine esters with high affinities and selectivities at diazepam insensitive (DI) benzodiazepine receptors. *J. Med. Chem.* 1001–1006.
(38) Ananthan, S.; Clayton, S. D.; Ealick, S. E.; Wong, G.; Evoniuk, G. E.; Skolnick, P. Synthesis and structure-activity relationships of 3,5-disubstituted 4,5-dihydro-6H-imidazo[1,5a][1,4]benzodiazepin-6-ones at diazepam-sensitive and diazepam-insensitive receptors. *J. Med. Chem.* **1993**, *36*, 479–490.
(39) SHELXTL 3.0; Sheldrick, G. M.; University of Goettingen, 1981.
(40) Crystallographic computer programs. Ahmed, F. R.; Huber, C. P.; Pippy, M. E.; NRC-(2.8.10.12) World List of Computer Programs, 1966.